Analytical Study of Crosstalk Propagation in All-Optical Networks Using Perturbation Theory

Yvan Pointurier, Student Member, IEEE, and Maïté Brandt-Pearce, Senior Member, IEEE
Charles L. Brown Department of Electrical and Computer Engineering
University of Virginia

Abstract

The performance of current optical networks is inherently limited by the speed of electronic components and in particular by the electronic switches. A new generation of optical networks, referred to as all-optical networks, overcome this limitation by switching data entirely optically using all-optical crossconnects (OXCs). However, all-optical networks are prone to phenomena that are unknown to current optical networks with electrical regeneration: OXCs are subject to optical leaks, called crosstalk, resulting in unwanted components being added to transmitted signals, and this crosstalk is transmitted over very long paths without any signal regeneration. In this paper, we consider the interplay between fiber nonlinearity and crosstalk signals over long distance as the source of performance degradation, measured in terms of Q factor. We present an analytical crosstalk model for all-optical networks and give expressions for the performance degradation resulting from the joint propagation of a signal (using a Continuous Wave assumption and perturbation theory) and crosstalk in large networks. Analytical calculations required by this model are shown to be much less computationally intensive than simulations. Simulations are carried out to validate our analytical model and good agreement is found between the analytical model and simulations for wide ranges of parameters.

I. Introduction

All-optical networks have emerged as a solution to keep up with the always increasing throughput demand. In today's transport networks, data is transmitted over optical fibers and optical-electro-optical conversion is needed at the nodes to perform routing. These networks can achieve a throughput of up to several tens of Gbits/s using Wavelength Division Multiplexed (WDM) channels. Yet optical fibers have a potential capacity of several tens of terabits/s. Electronic switches are not able to sustain such transmission rates and have become complex and costly, making it necessary to replace them with all-optical switches where no electric conversion is needed at all. As discussed in [1], deploying such all-optical networks is promising but also challenging and novel issues have to be anticipated. Crosstalk impairment, which we study in this paper, is one such issue.

All-optical switches (Optical Crossconnects (OXCs) and optical add-drop multiplexers (OADMs)) remove the electrical conversion step in switching hardware. In addition to the gain in network data rate, all-optical switches are expected to become simpler to implement and therefore cheaper than their electrical counterparts. Moreover, all-optical switches allow for improved data rate flexibility in networks. All-optical switches have been the subject of much research in the past few years and some are already commercially available [2]. The goal of an all optical switch is to transmit an incoming signal arriving on a certain wavelength and from a certain optical fiber to a different optical fiber. Although several architectures have been proposed, all-optical switches contain the same functional elements: demultiplexers, a switching fabric, optional wavelength converters, and multiplexers as depicted in Fig. 1; we refer the reader to [3] for a comprehensive review of enabling technologies for all-optical networks, including several OXC architectures and numerical data for all-optical components parameters. In this paper, we do not consider wavelength conversion nor optical regenerators, as those devices are still at the experimental stage and are likely to be costly.

Within an OXC, signals can leak due to the physical imperfections of the components. The *crosstalk* phenomenon refers to the presence of unwanted components (*crosstalk signals*) at the output of the switch because of leaks of the input signal. More details about crosstalk, including its modeling and classification into broad classes, is available in [4] and [5]. For example, consider the OXC with n ports in Fig. 1, where we assume that channel λ_1 from the

This work was supported by the National Science Foundation under grant CCF-0311198.

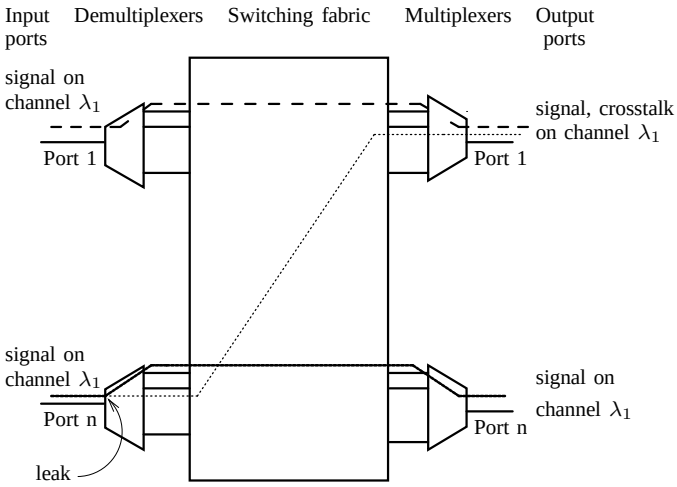

Fig. 1. **Source of in-band crosstalk.** Due to filter imperfection in the OXC, a small amount of the input signal on channel λ_1 on the n^{th} input port is allowed in the switching fabric via the input reserved for channel λ_2.

first input port is routed to the first output port, channel λ_1 from the n^{th} input port is routed to the n^{th} output port, and channel λ_2 from the n^{th} input port is routed to the first output port. In Fig. 1, a leak occurs in the n^{th} input demultiplexer that allows part of signal on channel λ_1 to leak, to travel with λ_2 within the switching fabric, and to be present at the output of the first output demultiplexer.

Crosstalk can be in-band (the crosstalk component and the input signal are on the same channel) or out-of-band (the channels are different). It is shown in [6] that in-band crosstalk accumulates much faster than out-of-band crosstalk while passing though the optical switches and has much more deleterious effects than in-band crosstalk at the detection stage, and therefore we consider in-band crosstalk only in this work. We still allow the in-band crosstalk component in a signal to be slightly detuned in frequency from the main signal because the crosstalk component and the main signal may not come from the same laser source [7], [8], [9].

In this paper, we study the performance degradation in all-optical transport networks caused by crosstalk originating from leaks in OXCs. Because of fiber nonlinearity and because signals are transmitted over long optical paths with no further regeneration or reshaping than amplification, crosstalk is a major impairment in all-optical networks, and thus crosstalk should be accounted for at the design stage when planning for all-optical network deployment. Availability of a fast method to assess crosstalk impairment in future all-optical networks is important in certain applications such as crosstalk-aware Routing and Wavelength Assignment algorithms design [10], [11].

Crosstalk accumulation, due to the concatenation of optical switches (ignoring transmission issues), is a well-known problem [6], [12]. The transmission of crosstalk has been studied in the past [4], [7], [8], [9], but not analytically. The primary focus of this work is on the analysis of the interplay between fiber physical parameters, especially fiber nonlinearity, and crosstalk. To the best of the authors' knowledge, the study of the transmission effects on crosstalk in nonlinear fibers for modulated signals has not been carried out analytically before. We present a new method based on perturbation theory to analytically compute the impact of crosstalk on the performance of all-optical networks. We assess the performance of a network via its *Q factor*, from which a bit error rate (BER) can be estimated. Our analysis assumes the transmission of a continuous wave signal (CW pump) perturbed by crosstalk, viewed as small signals. Under the continuous wave assumption, we are able to derive a fast and accurate means of studying signal transmission subject to crosstalk in optical fibers. Here, other impairments such as receiver noise, inter-channel interference, insertion loss due to the optical components, polarization mode dispersion (PMD), which have been studied in the past and could be incorporated in the model, are ignored for simplicity.

This paper is organized as follows. The system of interest is described in Section II. In Section III, we present a perturbation theory based analysis of the impact of in-band crosstalk in all-optical networks. Our analytical results are validated over a wide range of system parameters through simulation in Section IV. We offer conclusions in Section V.

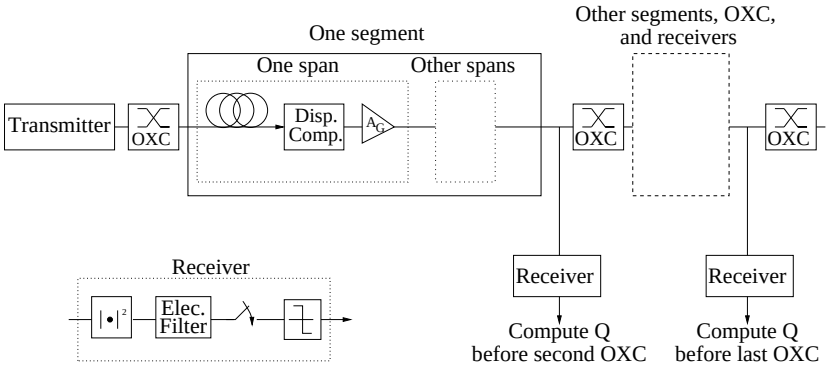

Fig. 2. **Simulated network.** Each OXC adds a crosstalk component to the input signals.

II. System description

A. Network model

To carry out our analysis and simulations, we model a path in an all-optical network as depicted in Fig. 2. The transmitter generates a CW signal with power P_0 in the analytical section, and a modulated signal with peak power P_0 in the simulation section. The path consists of N_s *segments* separated by OXCs that inject crosstalk in the system; we describe crosstalk modeling in Section II-B. Each segment consists in turn of a fixed number N_f of fiber *spans* of length L. (We assume that the number of spans is the same for each segment to simplify the notations, but generalization to different span numbers per segment can easily be included in our analysis.) In each fiber span, an optical amplifier with gain A_G compensates exactly for the fiber loss and dispersion compensation may be used as depicted in Fig. 2.

The main signal and the crosstalk signals propagate from one end of the path to the other; the propagation equation of an optical signal with slowly varying complex envelope $A = A(t, z)$ at time t and position z along a fiber is given by the nonlinear Schrödinger equation [13]:

$$\frac{\partial A}{\partial z} = -\frac{\alpha}{2}A + \frac{j}{2}\beta_2\frac{\partial^2 A}{\partial t^2} - j\gamma\left|A\right|^2 A \tag{1}$$

where α is the linear attenuation, β_2 the second-order dispersion, and γ nonlinear parameter. Again, in our analysis, we assume that all fiber spans of the path are physically identical but generalization to path which contain different types of fiber is straightforward.

We assess the performance of the path via its *Q factor*. The Q factor is an electrical SNR expression related to the bit error rate (BER) of the system ($BER = \frac{1}{2}\mathrm{erfc}\frac{Q}{\sqrt{2}}$) under a Gaussian assumption which is more accurate as the number of crosstalk signals grows [14]. We calculate the Q factor at the output of (virtual) receivers placed at the end of each span. Since each OXC injects new crosstalk, by placing the receivers before an OXC, we are able to assess the impact of fiber crosstalk on the path performance without having to account for crosstalk components injected by subsequent OXCs on the path. Each receiver is modeled by an ideal photodetector (a square-law detector), an electrical filter with narrow bandwidth, and a sampler. The Q factor can be calculated as $Q = (\mu_1 - \mu_0)/(\sigma_0 + \sigma_1)$ where μ_0, μ_1 are the means of the received samples corresponding to (sent) zeros and ones respectively, and σ_0 and σ_1 are the standard deviations. The CW assumption approximates NRZ modulation where "one" bits are sent.

In this work, we account for crosstalk as a noise term in the variance σ_1^2 [14]. Using this model, we further assume that the effects of signal-signal and signal-crosstalk nonlinear transmission are independent and therefore the variance σ_1^2 can be split into two terms: $\sigma_1^2 = \sigma_i^2 + \sigma_x^2$, one corresponding to the ISI and linear and nonlinear propagation effects on the main signal due to its transmission through the fiber (σ_i^2) and the other term due to the crosstalk (σ_x^2). We estimate μ_0, μ_1, σ_0 and σ_i using a simulation of the transmission of a short pseudo-random sequence of bits through the modeled network. It is also possible to estimate the crosstalk variance σ_x^2 by Monte-Carlo simulation, but doing so is a time-consuming technique due to the large number of random variables (bits, phase, delay) to consider. We present here a faster, analytical technique to compute σ_x^2.

Because our main interest lies in the study of the interactions between fiber properties and detuned crosstalk, we assume that amplifiers do not add any noise to the signal. In this paper, we do not consider inter-channel

interactions (which can be included using, for instance, the Volterra Series Transfer Function approach as in [15]) and therefore consider a single-channel system.

B. Crosstalk model

After describing the physical and topological properties of the system of interest, we now describe our crosstalk modeling. At each OXC, the main signal is corrupted by a certain number of crosstalk signals. We first consider a single crosstalk signal, and then extend our analysis to several crosstalk terms. Since the crosstalk component and the input signal come from two different sources, the crosstalk can be slightly detuned from the main signal by an angular frequency ω_s. Crosstalk signals are caused by, among other reasons, filter imperfections in OXCs and are therefore very attenuated versions of signals transmitted on other links.

The polarization between the main signal and the crosstalk signal is random; however, it was shown in [16] that impairments due to crosstalk are dominated by the case where the main and the crosstalk signals are in the same polarization state, and hence systems should be designed for this worst case. In this paper, we therefore assume that the main signal and the crosstalk signal are copolarized.

We call η the peak power ratio of the crosstalk to the main signal peak power. In practice, η is as high as -25 dB in Fiber Bragg Grating (FBG) based switches which integrate the demultiplexing and the spatial switching functionalities in the same fabric. Although crosstalk can be lower than -60 dB for MEMs spatial switches that are used in commercial all-optical switches, in such switches crosstalk originates from the multiplexing/demultiplexing stages and can amount to -20 dB [3], [17].

Given a baseband pulse shape $h(t)$ for the transmitted (crosstalk) bits, normalized to unit amplitude, we write the complex envelope of the fiber input signal $s_0(t)$ as the sum of the main signal (a CW pump) and a crosstalk bit:

$$s_0(t) = \sqrt{P_0} + m g_0(t-\tau), \tag{2}$$

where m is 0 or 1 with equal probability, and $g_0(t)$ is the effective transmit pulse shape

$$g_0(t) = \sqrt{\eta P_0} h(t) e^{j\omega_s t + j\varphi}. \tag{3}$$

The phase φ and the delay τ of the crosstalk with respect to the input signal are assumed to be randomly distributed, respectively between 0 and 2π, and 0 and the bit duration T_b.

The goal of the following section is to obtain an analytical expression for the crosstalk variance of the output signal at different points along the network when $s_0(t)$ is taken as the input.

III. Analysis

A. Crosstalk impact in single-segment systems

In this section, we apply perturbation theory results to the transmission of a CW signal perturbed by a small crosstalk signal. We focus on a single-segment path of N_f fiber spans between 2 OXCs. A CW pump and a single crosstalk component are injected by the first OXC, and the signal is observed just before the second OXC so that we can ignore the impact of the second OXC on the system for now; how to deal with several OXCs is discussed in the next section.

Perturbation theory has successfully been applied to the study of transmission impairments due to noise [18], [19], [20] and fiber nonlinearity [21]. We consider only first-order interactions, that is, interactions between the CW pump and crosstalk, and neglect all higher order interactions such as crosstalk-crosstalk interaction. Since crosstalk can be considered as a small perturbation to the CW pump, previously published results hold. In this section, we first determine the pulse shape of a crosstalk bit after transmission through a nonlinear fiber, and then use this pulse shape to compute the variance σ_1 needed to determine the Q factor of a path in an all-optical network.

First we rewrite the signal $s_0(t) = \sqrt{P_0} + m g_0^I(t) + jm g_0^Q(t)$, where we split a crosstalk bit (detuned by ω_s, delayed randomly by τ and with the constant but random phase φ relatively to the CW pump) $g_0(t)$ into an in-phase term $g_0^I(t)$ and a quadrature term $g_0^Q(t)$ with respect to the CW pump phase. Suppose the input signal is transmitted through k spans. We denote by $g_k(t)$ and $G_k(\omega)$ the pulse shape of the crosstalk bit at the output of the k^{th} span

in the time and frequency domain respectively, and by g_k^I and g_k^Q the in-phase and quadrature pulse shapes relative to the output CW signal. The signal at the output of the kth span $s_k(t)$ can be written as:

$$\begin{aligned} s_k(t) &= \sqrt{P_0}e^{jk\theta_{SPM}} + mg_k(t-\tau) && (4)\\ &= e^{jk\theta_{SPM}}\left(\sqrt{P_0} + m\left(g_k^I(t-\tau) + jg_k^Q(t-\tau)\right)\right), && (5)\end{aligned}$$

where $\theta_{SPM} \approx -\frac{\gamma P_0}{\alpha}$ is the rotation of the CW pump phase under Self-Phase Modulation (SPM), assuming $e^{-\alpha L} \ll 1$.

Now, $g_k^I(t)$ and $g_k^Q(t)$ can be split into 2 terms corresponding to conjugate terms, both independent of φ, such that:

$$g_k^I(t) = g_k^{I+}(t)e^{j\varphi} + g_k^{I-}(t)e^{-j\varphi} = \mathcal{F}^{-1}\left(G_k^{I+}(\omega)\right)e^{-j\varphi} + \mathcal{F}^{-1}\left(G_k^{I-}(\omega)\right)e^{j\varphi}, \quad (6)$$

$$g_k^Q(t) = g_k^{Q+}(t)e^{j\varphi} + g_k^{Q-}(t)e^{-j\varphi} = \mathcal{F}^{-1}\left(G_k^{Q+}(\omega)\right)e^{-j\varphi} + \mathcal{F}^{-1}\left(G_k^{Q-}(\omega)\right)e^{j\varphi} \quad (7)$$

where $\mathcal{F}^{-1}$ denotes the inverse Fourier transform operator.

Small perturbation theory is now utilized to give a linear relation between the terms making up the output of the fiber span $G_k^{I+}(\omega)$, $G_k^{Q+}(\omega)$, $G_k^{I-}(\omega)$, $G_k^{Q-}(\omega)$ and those of the input of the fiber span $G_{k-1}^{I+}(\omega)$, $G_{k-1}^{Q+}(\omega)$, $G_{k-1}^{I-}(\omega)$, $G_{k-1}^{Q-}(\omega)$ in the frequency domain via a *transfer matrix* $T_k(\omega)$:

$$\begin{bmatrix} G_k^{I+}(\omega) \\ G_k^{Q+}(\omega) \end{bmatrix} = T_k(\omega)\begin{bmatrix} G_{k-1}^{I+}(\omega) \\ G_{k-1}^{Q+}(\omega) \end{bmatrix}, \begin{bmatrix} G_k^{I-}(\omega) \\ G_k^{Q-}(\omega) \end{bmatrix} = T_k(\omega)\begin{bmatrix} G_{k-1}^{I-}(\omega) \\ G_{k-1}^{Q-}(\omega) \end{bmatrix}. \quad (8)$$

Moreover, it can be shown that [19]:

$$T_k(\omega) = \begin{bmatrix} \frac{1}{2}e^{-j\theta_{SPM}} & \frac{1}{2}e^{j\theta_{SPM}} \\ \frac{1}{2j}e^{-j\theta_{SPM}} & -\frac{1}{2j}e^{j\theta_{SPM}} \end{bmatrix}\mathcal{D}(\omega)\mathcal{M}(\omega)\begin{bmatrix} 1 & j \\ 1 & -j \end{bmatrix}, \quad (9)$$

where:

$$\mathcal{M}(\omega) = \begin{bmatrix} \mathcal{M}_{1,1}(\omega) & \mathcal{M}_{1,2}(\omega) \\ \mathcal{M}_{1,2}^*(\omega) & \mathcal{M}_{1,1}^*(\omega) \end{bmatrix}, \quad (10)$$

$$\mathcal{M}_{1,1}(\omega) = e^{-\frac{\alpha}{2}L}A_G e^{-\frac{j}{2}\beta_2 L\omega^2}\left(1 - j\frac{2\gamma P_0}{\alpha} + \frac{\gamma^2 P_0^2}{2\alpha(\alpha - j\beta_2\omega^2)} - \frac{2\gamma^2 P_0^2}{\alpha^2}\right), \quad (11)$$

$$\mathcal{M}_{1,2}(\omega) = e^{-\frac{\alpha}{2}L}A_G e^{-\frac{j}{2}\beta_2 L\omega^2}\left(-j\frac{\gamma P_0}{\alpha - j\beta 2\omega^2} - \frac{2\gamma^2 P_0^2}{\alpha(2\alpha - j\beta_2\omega^2)}\right). \quad (12)$$

The transmission matrix $\mathcal{M}$ accounts for linear and nonlinear effects during the transmission, and $\mathcal{D}$ accounts for post-dispersion compensation, if any. If no post-dispersion compensation is provided then $\mathcal{D}(\omega)$ is equal to the 2×2 identity matrix $I_{2\times 2}$; otherwise

$$\mathcal{D}(\omega) = \begin{bmatrix} e^{\frac{j}{2}\beta_2 L_d\omega^2} & 0 \\ 0 & e^{-\frac{j}{2}\beta_2 L_d\omega^2} \end{bmatrix}, \quad (13)$$

where L_d is the amount of compensation provided by the dispersion compensators, that is, the fiber length for which compensation is provided. If pre-dispersion compensation is used instead of post-dispersion compensation, then the order of the $\mathcal{D}$ and $\mathcal{M}$ matrices has to be reversed.

We can extend this result to the transmission through k spans:

$$\begin{bmatrix} G_k^{I+}(\omega) \\ G_k^{Q+}(\omega) \end{bmatrix} = T_k(\omega)\dots T_1(\omega)\begin{bmatrix} G_0^{I+}(\omega) \\ G_0^{Q+}(\omega) \end{bmatrix}, \begin{bmatrix} G_k^{I-}(\omega) \\ G_k^{Q-}(\omega) \end{bmatrix} = T_k(\omega)\dots T_1(\omega)\begin{bmatrix} G_0^{I-}(\omega) \\ G_0^{Q-}(\omega) \end{bmatrix}. \quad (14)$$

Here, the inputs $G_0^{I+}(\omega)$, $G_0^{Q+}(\omega)$, $G_0^{I-}(\omega)$ and $G_0^{Q-}(\omega)$ are given as a function of the input pulse shape ($h(t)$) in the frequency domain $H(\omega)$ by:

$$G_0^{I+}(\omega) = \sqrt{\eta P_0}\frac{e^{-j\omega\tau}}{2}H(\omega - \omega_s), G_0^{I-}(\omega) = \sqrt{\eta P_0}\frac{e^{-j\omega\tau}}{2}H(\omega + \omega_s), \quad (15)$$

$$G_0^{Q+}(\omega) = \sqrt{\eta P_0}\frac{e^{-j\omega\tau}}{2j}H(\omega-\omega_s), G_0^{Q-}(\omega) = -\sqrt{\eta P_0}\frac{e^{-j\omega\tau}}{2j}H(\omega+\omega_s). \quad (16)$$

We now determine the crosstalk variance σ_x^2. We denote by $f(t)$ the electrical filter impulse response and by $*$ the convolution operation. We call ρ the responsivity of the square-law detector. Since the crosstalk pulse shape after k spans can be written as:

$$g_k(t) = (g_k^{I+}(t)e^{j\varphi} + g_k^{I-}(t)e^{-j\varphi}) + j(g_k^{Q+}(t)e^{j\varphi} + g_k^{Q-}(t)e^{-j\varphi}), \quad (17)$$

then the current $i(t,k)$ that corresponds to the power distortion due to the presence of crosstalk in the system is, at the output of the k^{th} span and after photodetection:

$$\begin{aligned}
i(t,k) &= \rho f(t) * \left(\left| \sqrt{P_0}e^{jk\theta_{SPM}} + m g_k(t-\tau) \right|^2 - P_0 \right) && (18)\\
&= \rho f(t) * \Big(\Big| \sqrt{P_0}e^{jk\theta_{SPM}} + m\Big((g_k^{I+}(t-\tau)e^{j\varphi} + g_k^{I-}(t-\tau)e^{-j\varphi}) \\
&\qquad + j(g_k^{Q+}(t-\tau)e^{j\varphi} + g_k^{Q-}(t-\tau)e^{-j\varphi})\Big) e^{jk\theta_{SPM}} \Big|^2 - P_0 \Big) && (19)\\
&= \rho f(t) * \Big(2\sqrt{P_0} m \left(g_k^{I+}(t-\tau)e^{j\varphi} + g_k^{I-}(t-\tau)e^{-j\varphi} \right) \\
&\qquad + \Big(m\Big((g_k^{I+}(t-\tau)e^{j\varphi} + g_k^{I-}(t-\tau)e^{-j\varphi}) \Big)^2 \\
&\qquad + \Big(m\Big((g_k^{Q+}(t-\tau)e^{j\varphi} + g_k^{Q-}(t-\tau)e^{-j\varphi}) \Big)^2 \Big) && (20)\\
&\approx 2\rho\sqrt{P_0} m f(t) * \left(g_k^{I+}(t-\tau)e^{j\varphi} + g_k^{I-}(t-\tau)e^{-j\varphi} \right) && (21)
\end{aligned}$$

in a first-order approximation, neglecting the squared crosstalk term and ISI between the crosstalk bits. We now take the variance of this quantity with respect to the random delay τ, phase ϕ, and bits m:

$$\begin{aligned}
\sigma_x^2(t,k) &= Var_{m,\tau,\varphi}[i(t,k)] && (22)\\
&= E_\tau E_m E_\varphi \left[(i_k(t))^2 \right] - E_\tau E_m E_\varphi \left[i_k(t) \right]^2 && (23)\\
&= E_\tau E_\varphi E_m \left[\left(2\rho\sqrt{P_0} m f(t) * (g_k^{I+}(t-\tau)e^{j\varphi} + g_k^{I-}(t-\tau)e^{-j\varphi}) \right)^2 \right] && (24)\\
&= 2\rho^2 P_0 E_\tau E_\varphi \Big[\left(f(t) * g_k^{I+}(t-\tau) \right)^2 e^{2j\varphi} + \left(f(t) * g_k^{I-}(t-\tau) \right)^2 e^{-2j\varphi} \\
&\qquad + 2 \left(f(t) * g_k^{I+}(t-\tau) \right) \left(f(t) * g_k^{I-}(t-\tau) \right) \Big] && (25)\\
&= 4\rho^2 P_0 E_\tau \left[|f(t) * g_k^{I+}(t-\tau)|^2 \right], && (26)
\end{aligned}$$

since $E_\varphi \left[i_k(t) \right] = 0$, using the distributions of m and φ and noticing that $g_k^{I+}(t)$ and $g_k^{I-}(t)$ are complex conjugates. Finally, the expectation with regards to time delay τ can be computed as:

$$\sigma_x^2(t,k) = 4\rho^2 P_0 \int_{-\infty}^{\infty} \frac{1}{T_b} |f(t) * g_k^{I+}(t-\tau)|^2 \mathrm{d}\tau, \quad (27)$$

extending the integral from $[0, T_b]$ to $[-\infty, \infty]$ to account for crosstalk ISI. Finally, at the end of the path, after N_f spans:

$$\sigma_x^2 = \sigma_x^2(T_b/2, N_f) = 4\rho^2 P_0 \int_{-\infty}^{\infty} \frac{1}{T_b} |f(t) * g_{N_f}^{I+}(t)|^2 \mathrm{d}t. \quad (28)$$

This analysis can be extended to the case where the OXC adds several crosstalk signals, possibly with different attenuations and detunings. Indeed, since the crosstalk signals come from different sources, their phases, delays and bit patterns are independent and thus the variance of the overall crosstalk signal is simply obtained by adding the variances corresponding to the transmission of each crosstalk signal taken individually.

TABLE I
COMPLEXITY ANALYSIS PARAMETERS

Symbol	Meaning
N_s	Number of segments
N_f	Number of spans per segment
N_z	Number of trunks per span
N_r	Number of bit frames simulated
N_b	Number of bits in the bit frames
N_{spb}	Number of samples per bit

B. Multi-segment system

We now derive the expression for the system performance in the multi-segment case, as an extension of the single-segment case. Because the crosstalk signals added by each OXC are independent of each other and of every other crosstalk signal introduced by any other OXC, we can simply add their variances. As in the previous section, we consider the case where each OXC introduces a single crosstalk signal. We are interested in the variance of the current distortion just before the $(N_s+1)^{th}$ OXC.

We examine in turn the contribution to the current distortion variance of the crosstalk signal injected by each OXC. The crosstalk signal injected by the i^{th} OXC travels through all of the $(N_s-i+1)N_f$ spans between the i^{th} and the last OXC in the path, so the contribution of this crosstalk signal to σ_1^2 is $4P_0\rho^2 \int_{-\infty}^{\infty} \frac{1}{T_b}|f(t)*g^{I+}_{(N_s-i+1)N_f}(t)|^2\mathrm{d}t$. By independence of the crosstalk terms, the variance σ_x^2 due to crosstalk at the end of the path is given by the sum of these contributions and:

$$\sigma_x^2 = \sum_{i=1}^{N_s} 4P_0\rho^2 \int_{-\infty}^{\infty} \frac{1}{T_b}|f(t)*g^{I+}_{(N_s-i+1)N_f}(t)|^2\mathrm{d}t. \tag{29}$$

We can easily extend this result to the case where each OXC adds more than one crosstalk signal, possibly with different parameters such as crosstalk attenuation or detuning, considering that all crosstalk components are independent from each other (since they come from different sources).

We have presented an analytical method to compute the Q factor of a path in a network subject to crosstalk; we now show that this method is less computationally expensive than simulation.

C. Complexity analysis

In this section, we compare the computational time complexity of our algorithm with that of the conventional method which simulate signal propagation in fiber optics.

The conventional method used to compute the Q factor of the systems of interest involves performing Monte Carlo simulations and solving the nonlinear Schrödinger equation numerically with the Split-Step Fourier method (SSF) [13]. We assume for simplicity that we want to compute the Q factor for a path of N_s segments, where each segment is N_f spans long. Additionally, the SSF algorithm splits each span into N_z smaller trunks; the number of trunks is dependent on both the span length and the signal parameters. More specifically, a larger number of trunks are required for higher signal powers. Each bit is sampled N_{spb} times, and we simulate the transmission of N_r frames of N_b bits each; each frame has its own random crosstalk bits, phase and delay. These parameters are summarized in Table I.

Consider Monte Carlo simulations first. The SSF mainly consists of FFTs, hence a complexity of $N_{spb}N_b\log(N_{spb}N_b)$ per frame. We need to perform N_r SSF per span trunk and there are $N_zN_sN_f$ span trunks in the path, so the overall time complexity is in the order of $N_zN_rN_sN_fN_{spb}N_b\log(N_{spb}N_b)$.

Now consider our analytical method. Our analytical method requires to simulate the transmission of one frame through the system to estimate μ_0, μ_1, σ_0, σ_i. This is done in time $N_zN_sN_fN_{spb}N_b\log(N_{spb}N_b)$. Then, we convert the signal from time to frequency domain (complexity: $N_{spb}N_b\log(N_{spb}N_b)$). Computing each T_k matrix is done in time $N_{spb}N_b$ (we need one matrix multiplication per sample in the frequency domain), and we need N_sN_f multiplications to compute the pulse shape of the crosstalk component introduced by the first OXC, $(N_s-1)N_f$ for the crosstalk component introduced by the second OXC, etc. Overall we need $N_s^2N_f$ matrix multiplications,

TABLE II
BASELINE SYSTEM PARAMETERS

Parameter	Description	Baseline Value	Range tested
N_s	Number of segments	1	1 – 4
N_f	Number of fiber spans per segment	10	3 – 12
L	Span length	100 km	
P_0	Pump power	2 mW	1 – 10 mW
T_b	Crosstalk bit duration	100 ps (10 Gbps)	2.5, 10 Gbps
	Pulse shape	Super-Gaussian NRZ	
η	Crosstalk attenuation (power)	-30 dB	-30 – -15 dB
ω_s	Crosstalk detuning	0 GHz	0 – 8 GHz
α	Fiber loss	0.2 dB/km	
γ	Nonlinear coefficient	2.2 (W km)$^{-1}$	
D	Second order linear dispersion	17 ps/nm/km (SMF)	
L_D	Dispersion compensation length	100 km	0, 100 km
NF	Noise parameter	0 (no noise)	0, 2
ρ	Photodetector responsitivity	1 A/W	
	Photodetector bandwidth	$0.7/T_b$	

which takes time $N_s^2 N_f N_{spb} N_b$, to get the pulse shapes of the crosstalk signals introduced by all OXCs. Addition and integration of each of the N_s pulse shapes (Eq. 29) is done in time $N_s N_{spb} N_b$, which is negligible with respect to the time taken to compute the pulse shapes. Overall the crosstalk analysis time complexity is $N_s N_f N_{spb} N_b (N_z \log(N_{spb} N_b) + N_s)$.

In practice, computing Q through analysis is several thousands times faster than through simulation, because N_r has to be large: we need values of N_r of several thousands to get reliable values of Q because we must average the performance over three independent random variables.

IV. VALIDATION BY SIMULATION

A. Baseline system

In this section, we seek to validate with Monte Carlo simulations our analytical approach and to determine its limits over a wide range of physical parameters.

We use the following numerical values for a baseline path from which all of our modeled paths are simulated. For all plots, one or two parameters are varied, leaving the others as described here. These parameters are chosen to model large-scale metropolitan to continental networks. The path consists of a single segment of 10 spans of SMF (single mode fiber, $D = -\beta_2 \nu^2/(2\pi c)$=17 ps/nm/km) with nonlinear coefficient γ=2.2 W^{-1}km^{-1}. Each span is 100 km long. Amplifiers compensate exactly for the fiber loss (0.2 dB/km) and do not introduce any noise. Post-dispersion compensation is provided after each span and is assumed to compensate exactly for the SMF dispersion. The length of the dispersion compensating fibers is neglected. The peak power of the transmitted signal with no crosstalk is P_0=2 mW and the power attenuation of the unique crosstalk signal introduced by the first OXC is -30 dB. Main signal and crosstalk are a frame of NRZ super-Gaussian pulses not detuned from the main signal (f_s=$\omega_s/(2\pi)$=0 GHz). These parameters are summarized in Table II. In each simulation, we transmit 2048 frames of 16 pulses, varying the phase and delay between the frames, to ensure tight confidence intervals on the Q factor (confidence interval tighter than 0.2 for Q≈6). We simulate the transmission of a single frame of 16 bits to estimate μ_1, μ_0, σ_0, σ_i. In each of the following plots, plain lines are obtained using the analytical model and dotted lines come from simulations.

In the systems we simulate, since the main signal is modulated and its peak power varies slightly with the transmission distance. To account for this variation in the estimation of σ_x, we replace P_0 in (28) by the value of μ_1 obtained from this short simulation, such that:

$$\sigma_x^2 = 4\mu_1 \rho^2 \int_{-\infty}^{\infty} \frac{1}{T_b} |f(t) * g_{N_f}^{I+}(t)|^2 \mathrm{d}t. \tag{30}$$

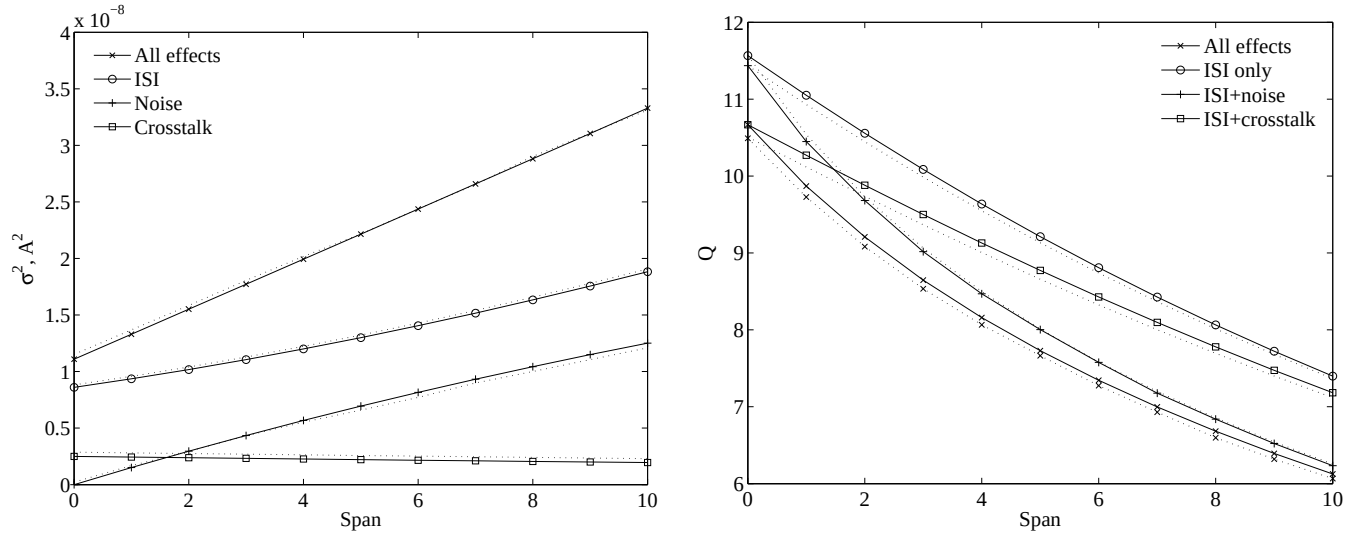

(a) Variance (b) Q factor

Fig. 3. Details of the impact of each impairment on a 10 GHz dispersion-compensated system: noise, ISI, crosstalk.

B. Effects of fiber and crosstalk parameters

In the first simulation, we seek to verify that the CW assumptions and the transmission effects on the main signal (accounted for by σ_i^2), the noise (accounted for by σ_n^2) and the impairment due to crosstalk (accounted for by σ_x^2) are independent, such that $\sigma_1^2 = \sigma_i^2 + \sigma_n^2 + \sigma_x^2$. We also verify that simulating the propagation of a single frame is enough to estimate μ_1, μ_0, σ_0 and σ_i.

First consider Fig. 3(a), where the variances for transmission effects on the main signal, noise, and crosstalk, are plotted at the output of each span of our baseline network. For this case we consider that the optical amplifier after each span injects noise in the network. The analytical curves for crosstalk was obtained using the results of Section III. The analytical curve for σ_n^2 was obtained using [19]. The "analytical" curve for σ_i^2 is actually the estimate obtained by a single-frame transmission simulation. The analytical curve for all effects combined (σ_1^2) was obtained by summing up the variances σ_i^2, σ_n^2, σ_x^2. The simulation curve for σ_1^2 was obtained by full-length Monte-Carlo simulation including random crosstalk and noise. We then ran three additional Monte-Carlo simulation: one with no crosstalk and no noise (from which we obtained the plot for σ_i^2), one with crosstalk but no noise, and one with noise but no crosstalk to deduce the plots for σ_x^2 and σ_n^2.

The simulation (dotted) and analytical (plain) plots agree very well, after each span, for all the cases we consider — noise only, crosstalk only, transmission effects only, and all effects combined. For these parameters, σ_x^2 from (30) slightly underestimates the crosstalk variance. In this dispersion compensated network, all effects have the same order of magnitude, although we consider only a single crosstalk component. It is easy to see that crosstalk can dominate after transmission through only a few OXCs. Also, in this case, crosstalk variance tends to decrease with the transmission distance, thereby alleviating the impact of crosstalk as compared with other transmission impairments. This is caused by the tight electrical filter that removes part of the crosstalk spectrally spread by the fiber nonlinearity. In Fig. 3(b), we provide the Q factors for the ISI only, ISI+noise, ISI+crosstalk, and ISI+noise+crosstalk cases. Since the values for μ_1, μ_0 and σ_0 are dependent on the transmission length, Q accounts for transmission effects better than σ_1 only. Again, very good agreement is found between simulation and our analytical results. For the single crosstalk component case which is considered in this paper, the Gaussian approximation is not accurate and overestimates the crosstalk variance and hence underestimates the Q factor [14]. Nevertheless, since our technique is valid for any number of crosstalk components, obtaining accurate values for the Q factor for only one crosstalk signal ensures the attainment of accurate values of Q and thus of the BER with our technique in more realistic multi-crosstalk signals cases.

In the following plots, we show that our technique holds for wide ranges of system parameters. In Fig. 4, we provide data for a 2.5 Gbps network with no dispersion compensation and no noise. In this case, the crosstalk is

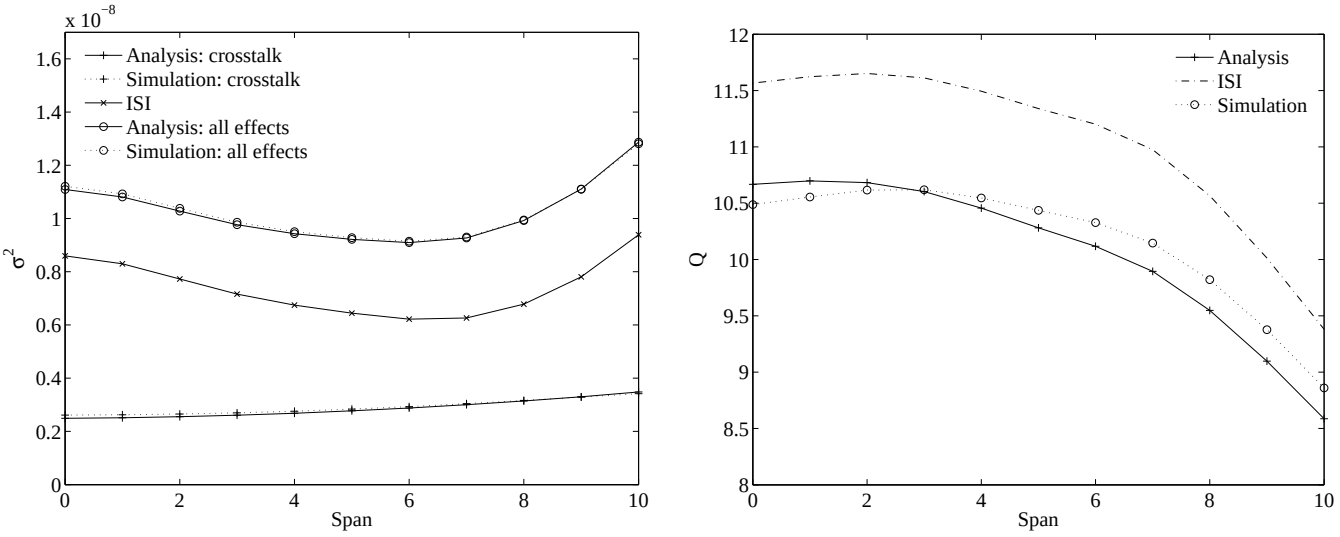

(a) Variance (b) Q factor

Fig. 4. Details of the impact of ISI and crosstalk on a 2.5 Gbps system.

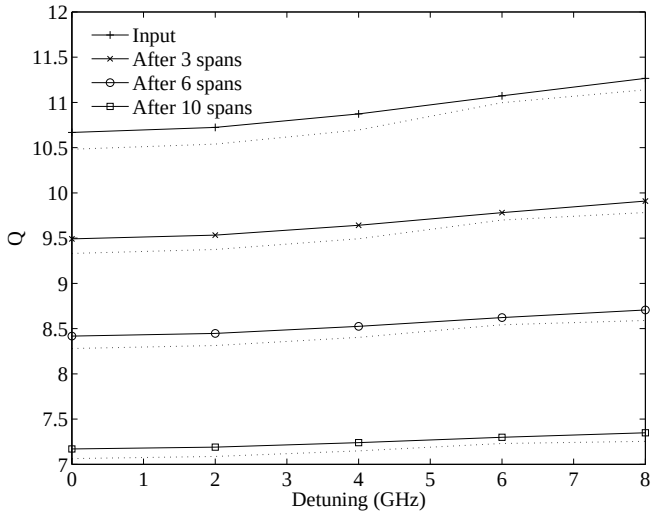

Fig. 5. Impact of detuning.

enhanced by the propagation through nonlinear fiber.

An important attribute of our analytical method is the ability to include the potential detuning f_s of the crosstalk signal with respect to the main signal power. Consider Fig. 5, where Q is plotted as a function of the detuning at several points in the network. We notice that Q is actually strongly dependent on the detuning, with higher values corresponding to higher detunings. This is expected because detuned crosstalk tends to be attenuated by the electrical filter. Other system parameters (square pulse shape, NZ-DSF fiber, high power) can lead to modulation instability at non-zero detuning levels [7], [8], [9]; our system does not exhibit this nonlinear phenomenon. Our model predicts the network performance well for the whole range of detunings. We did not consider higher detunings as highly detuned crosstalk can be filtered out.

In Fig. 6 and 7, we show that our technique is still valid for practical ranges of main signal powers and crosstalk attenuations despite the small signal approximation. We tested the analytical technique for main signal peak powers up to 10 mW; at such powers, nonlinear effects on the main signal dominate over crosstalk effects and the Q factor decreases below 6 after just a few spans. For lower powers, crosstalk is an important impairment and our analysis predicts the correct values for Q. Similarly, we predict accurate values for Q for crosstalk attenuation up to -20 dB;

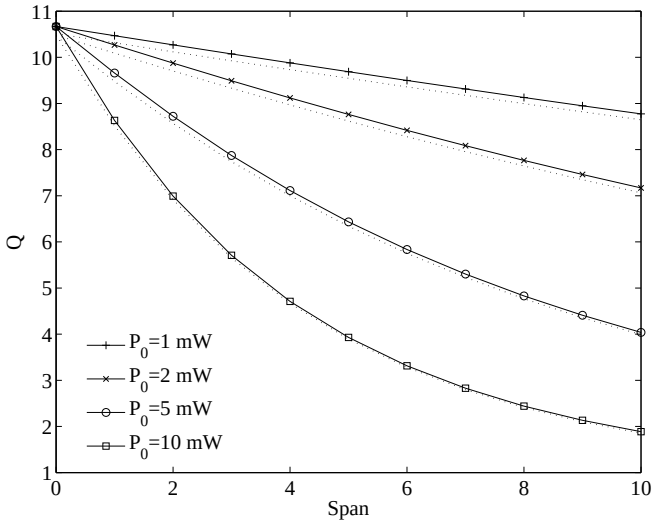

Fig. 6. Impact of the main signal peak power.

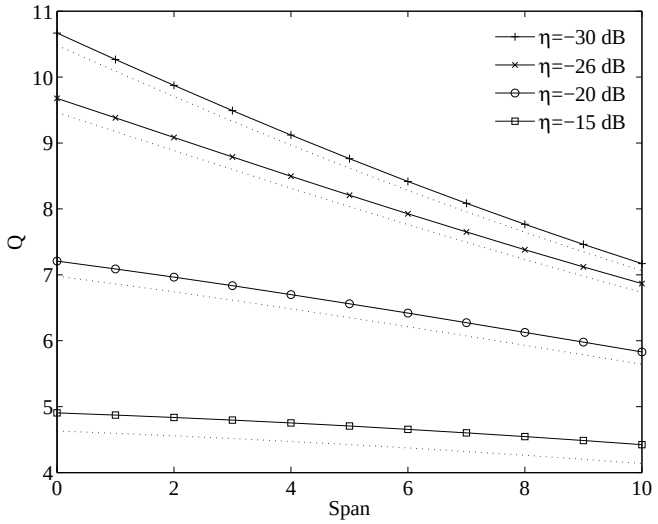

Fig. 7. Impact of the crosstalk attenuation.

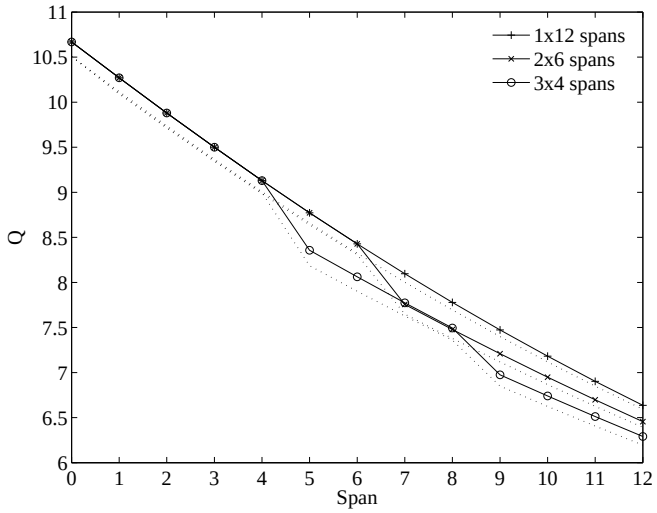

Fig. 8. Impact of the network topology.

if the crosstalk is stronger (-15 dB for instance), our approximations become inaccurate, but as seen on Fig.7, in such cases the Q factor is below 6 as early as the input of the first span (span "0", just after the first OXC) and therefore such situations are not of practical interest.

C. Effects of Network Topology

In this section, we consider a long path with total length fixed to 1200 km. Again, each OXC inserts a single crosstalk component and noise impact is ignored. We study the OXC insertion penalty on Q in the path. The following topologies are considered: a single segment of 12 spans, 2 segments of 6 spans each, and 3 segments of 4 spans each.

As shown in Fig. 8, the insertion of an OXC is clearly visible for every path topology and results in a sharp drop in the Q factor. The drop in Q is more pronounced after the first OXCs than after the last OXCs, because the marginal effect of adding one crosstalk term is largest at the beginning of the fiber. Again, our analytical model predicts the performance of such networks accurately.

V. Conclusion

In this paper, we develop a fast and accurate perturbation theory model for in-band crosstalk penalty by propagation through non-linear fiber. Our model holds for wide physical parameter ranges: power, crosstalk detuning and attenuation, presence of noise, network length and topology, presence of dispersion compensators. Model failure occurs only for extreme parameter values, which would not be used in real networks. Both OXC insertion and transmission effects have a strong negative impact on the Q factor, and neither can be overlooked when designing long haul or even metropolitan networks.

Only crosstalk effects have been accounted for, neglecting all other physical effects (insertion losses, inter-channel effects, PMD) to focus on the performance degradation due to crosstalk. However, other effects can be included in our analysis, for instance modeling those as additional variance terms as we have done for noise. We envision direct applications of our work to account for crosstalk impairments in routing and wavelength assignment problems and all-optical network design.

References

[1] B. Mukherjee, "WDM optical communication networks: Progress and challenges," *IEEE J. Select. Areas Commun.*, vol. 18, no. 10, pp. 1810–1824, Oct 2000.

[2] "Movaz networks." [Online]. Available: http://www.movaz.com/

[3] A. Willner, M. Cardakli, O. Adamczyk, Y.-W. Song, and D. Gurkan, "Key building blocks for all-optical networks," *IEICE Transactions on Communications*, pp. 2166–2177, Oct 2000.

[4] E. Iannone, R. Sabella, M. Avattaneo, and G. D. Paolis, "Modeling of in-band crosstalk in WDM optical networks," *J. Lightwave Technol.*, vol. 17, no. 7, pp. 1135–1141, Jul 1999.

[5] Y. Shen, K. Lu, and W. Gu, "Coherent and incoherent crosstalk in WDM optical networks," *J. Lightwave Technol.*, vol. 17, no. 5, pp. 759–764, May 1999.

[6] J. Zhou, R. Cadeddu, E. Casaccia, C. Cavazzoni, and M. O'Mahony, "Crosstalk in multiwavelength optical cross-connect networks," *J. Lightwave Technol.*, vol. 14, no. 6, pp. 1423–1435, Jun 1996.

[7] E. Ciaramella and F. Curti, "Impairments due to the interplay between node crosstalk and nonlinear propagation in all optical transport networks," *IEEE Photon. Technol. Lett.*, vol. 11, no. 5, pp. 563–565, May 1999.

[8] ——, "Experimental assessment of node crosstalk limitations enhanced by nonlinear effects in all optical transport networks," *IEEE Photon. Technol. Lett.*, vol. 11, no. 6, pp. 7511–753, Jun 1999.

[9] H. Kim and T. El-Bawab, "Enhancement of node-induced crosstalk by nonlinear effects in nonzero dispersion shifted-fiber rings with optical add-drop multiplexers," *Fiber and Integrated Optics, Taylor & Francis*, vol. 20, no. 6, pp. 625–635, 2001.

[10] T. Deng, S. Subramaniam, and J. Xu, "Crosstalk-aware wavelength assignment in dynamic wavelength-routed optical networks," in *First International Conference on Broadband Networks*, Oct 2004, pp. 140–149.

[11] Y. Pointurier and M. Brandt-Pearce, "Routing and wavelength assignment incorporating the effects of crosstalk enhancement by fiber nonlinearity," in *Proceedings of the 39th Annual Conference on Information Sciences and Systems (CISS), Baltimore, MD*, 2005.

[12] E. Goldstein and L. Eskildsen, "Scaling limitations in transparent optical networks due to low-level crosstalk," *IEEE Photon. Technol. Lett.*, vol. 7, no. 1, pp. 93–94, Jan 1995.

[13] G. Agrawal, *Nonlinear Fiber Optics*. Academic Press, 2001.

[14] H. Takahashi, K. Oda, and H. Toba, "Impact of crosstalk in an arrayed-waveguide multiplexer on NxN optical interconnection," *J. Lightwave Technol.*, vol. 14, no. 6, pp. 1097–1105, Jun 1996.

[15] B. Xu and M. Brandt-Pearce, "Comparison of FWM- and XPM-induced crosstalk using the Volterra Series Transfer Function method," *J. Lightwave Technol.*, vol. 21, no. 1, pp. 40–53, Jan 2003.

[16] E. Goldstein, L. Eskildsen, C. Lin, and Y. Silberberg, "Polarization statistics of crosstalk-induced noise in transparent lightwave networks," *IEEE Photon. Technol. Lett.*, vol. 7, no. 11, pp. 1345–1347, Nov 1995.

[17] S. Dods, J. Lacey, and R. Tucker, "Performance of WDM ring and bus networks in the presence of homodyne crosstalk," *J. Lightwave Technol.*, vol. 17, no. 3, pp. 388–396, Mar 1999.

[18] A. Carena, V. Curri, R. Gaudino, P. Poggiolini, and S. Benedetto, "New analytical results on fiber parametric gain and its effects on ASE noise," *IEEE Photon. Technol. Lett.*, vol. 9, no. 4, pp. 535–537, Dec 2001.

[19] B. Xu and M. Brandt-Pearce, "Analysis of noise amplification by a CW pump signal due to fiber nonlinearity," *IEEE Photon. Technol. Lett.*, vol. 16, no. 4, pp. 1062–1064, Apr 2004.

[20] G. Bosco, A. Carena, V. Curri, R. Gaudino, P. Poggiolini, and S. Benedetto, "A novel analytical approach to the evaluation of the impact of fiber parametric gain on the bit error rate," *IEEE Trans. Commun.*, vol. 49, no. 12, pp. 2154–2163, Dec 2001.

[21] M. Wu and W. Way, "Fiber nonlinearity limitations in ultra-dense WDM systems," *J. Lightwave Technol.*, vol. 22, no. 6, pp. 1483–1498, Jun 2004.